ELSEVIER

Journal of Marine Systems 18 (1998) 215–226

JOURNAL OF MARINE SYSTEMS

Estimating climatological age from a model-derived oxygen–age relationship in the Mediterranean

K. Stratford [a,*], R.G. Williams [a], P.G. Drakopoulos [b]

[a] *Oceanography Laboratories, Department of Earth Sciences, University of Liverpool, Liverpool L69 3BX, UK*
[b] *Department of Meteorology, University of Edinburgh, The King's Buildings, Edinburgh EH9 3JZ, UK*

Received 29 January 1996; accepted 4 November 1997

Abstract

Climatological oxygen observations suggest that the deep water of the western Mediterranean is better ventilated than that of the eastern Mediterranean. In this work, the oxygen distribution is modelled using an off-line tracer model driven by velocity fields from an eddy-permitting general circulation model. The model includes an air–sea transfer of oxygen, entrainment, and an interior oxygen consumption which varies in each basin according to estimates of the background new production. The modelled oxygen distribution shows higher values in the western basin when compared with the eastern basin, despite higher oxygen utilisation in the west, although the model underestimates the west–east contrast. In addition, an off-line ideal age integration is performed that shows ages reaching 100 yr in the eastern basin and 50 yr in the western basin, although the latter value should be viewed as an over-estimate as the modelled deep convection is too weak. These model integrations are combined to produce a relationship between the apparent oxygen utilisation (AOU) and age for each basin. A climatological age distribution is then inferred from the observed AOU distribution using the model-derived relationships. The predicted age reaches 80–120 yr and 20–40 yr in the bottom waters of the eastern and western basins respectively. The errors in this approach are likely to be significant, being ± 20 yr in the east and ± 40 yr in the west. However, the results are broadly in accord with independent estimates of overturning timescales—70 to 120 yr and 40 yr for the eastern and western basins, respectively.

Keywords: climatological age; oxygen–age relationship; Mediterranean

1. Introduction

The oxygen distribution has frequently been used to identify the pathway of fluid around ocean basins, as in the core analysis of Wüst (1935), as well as qualitatively to indicate the age of fluid as defined by the time since fluid was last at the surface. In practice, a quantitative calculation of the age from oxygen concentrations is rarely performed, as it requires assumptions to be made about the consumption of oxygen, along with the exact paths of fluid parcels and interior mixing. Despite these potential difficulties, Jenkins (1987) showed that there is a simple functional relationship between observations of apparent oxygen utilisation (AOU) and tritium–helium age in the upper thermocline of the beta

* Corresponding author. Present address: Southampton Oceanography Centre, Empress Dock, Southampton S0143ZH, UK. E-mail: kxs@soc.soton.ac.uk

0924-7963/98/$ - see front matter
PII: S0924-7963(98)00013-X

triangle site in the North Atlantic. He exploited this relationship to estimate the oxygen utilisation rate by estimating the advective oxygen supply from the horizontal gradients in AOU and the tritium–helium age.

In this study, we wish to follow a similar philosophy, but exploit the use of a general circulation model (GCM) to help understand the climatological oxygen distribution and deduce the implied age distribution. A straight-forward application of a GCM to understand tracer data is often difficult. The modelled tracer fields often appear unrealistic as a result of inaccuracies in the advecting circulation which are in turn caused by uncertainties in, for example, forcing and sub-grid scale parametrisations. However, a GCM can sometimes still be useful if the relevant controlling processes, such as the ventilation of the upper waters and transfer of water masses, are represented reasonably well. In this case, the GCM might provide better functional relationships between different tracers, than exact predictions of the geographic distribution of a single tracer.

In this study, a simple procedure is followed to understand the dissolved oxygen distribution and estimate the age of water from oxygen observations. First, climatological maps of oxygen concentration and AOU are constructed from observational data for the Mediterranean (Section 2). Second, the evolution of an idealised age tracer and of the oxygen concentration is determined using off-line tracer integrations driven by velocity fields from a seasonally-varying, eddy-permitting model of the Mediterranean; the model is described in Section 3 and the results in Section 4. The idealised age and oxygen distributions are both strongly dependent on the physical circulation, but have different source and sink terms associated with them. Separate functional relationships between the age and AOU are established for the western and eastern basins, since there are different levels of new production, and hence oxygen consumption, in each basin.

Finally, the implied age distribution is inferred from the climatological AOU distribution using the model derived functional relationship between age and AOU. This age distribution is discussed and compared with independent estimates in Section 5, along with the limitations and uncertainties inherent in the approach.

2. Climatological oxygen data

Oxygen data have been obtained from the MED2 historical data base (see Brasseur et al., 1996), which itself is a compilation of three separate data sets. The first is the BNDO (Bureau National des Donnees Oceaniques) set which consists of about 17,000 vertical profiles—mainly bottle data at original depths. These measurements were all collected after 1911, while the data set as a whole is representative of the 1945–1978 period. The second is the NODC (National Oceanographic Data Centre) which includes over 20,000 profiles interpolated to standard levels. The final source was the IRPEM (Instituto per la Ricerca sulla Pesca Maritima) data set made up of around 4000 stations mainly in the Adriatic Sea. This merged data set also provides observed temperature and salinity for the estimation of oxygen solubility in addition to the measured oxygen concentration.

These raw data have been processed here so that smooth fields are available on the same grid as is used by the model, employing a mapping technique based on a spatially weighted averaging procedure. Initially, a linear interpolation of values in the vertical was performed, onto the 19 depth levels of the model. Next, the observations were binned in $0.25^\circ \times 0.25^\circ$ latitude/longitude boxes at exactly the same co-ordinates as the model tracer grid. This was achieved by applying a two-dimensional moving average filter subject to the constraint that there be at least 10 raw data points within the averaging range. Thus, for example, if an area of four grid points contained fewer than 10 raw data points, the averaging was extended to encompass 16 boxes, and so on until a maximum of 100 boxes was reached. In this way one obtains a varying resolution ranging from $0.5^\circ \times 0.5^\circ$ down to a minimum of $2.5^\circ \times 2.5^\circ$. In order to avoid extensive leakage of features between adjacent locations, data were averaged with a weight proportional to the square of the inverse distance between their position and the grid point of interest.

2.1. Oxygen and AOU distributions

Fig. 1 shows the annual average oxygen concentration and AOU distributions on the 1500 m isobath, which is typical for the mid-depth and deep waters. It can be seen that the oxygen concentrations are generally higher in the western basin, where one sees

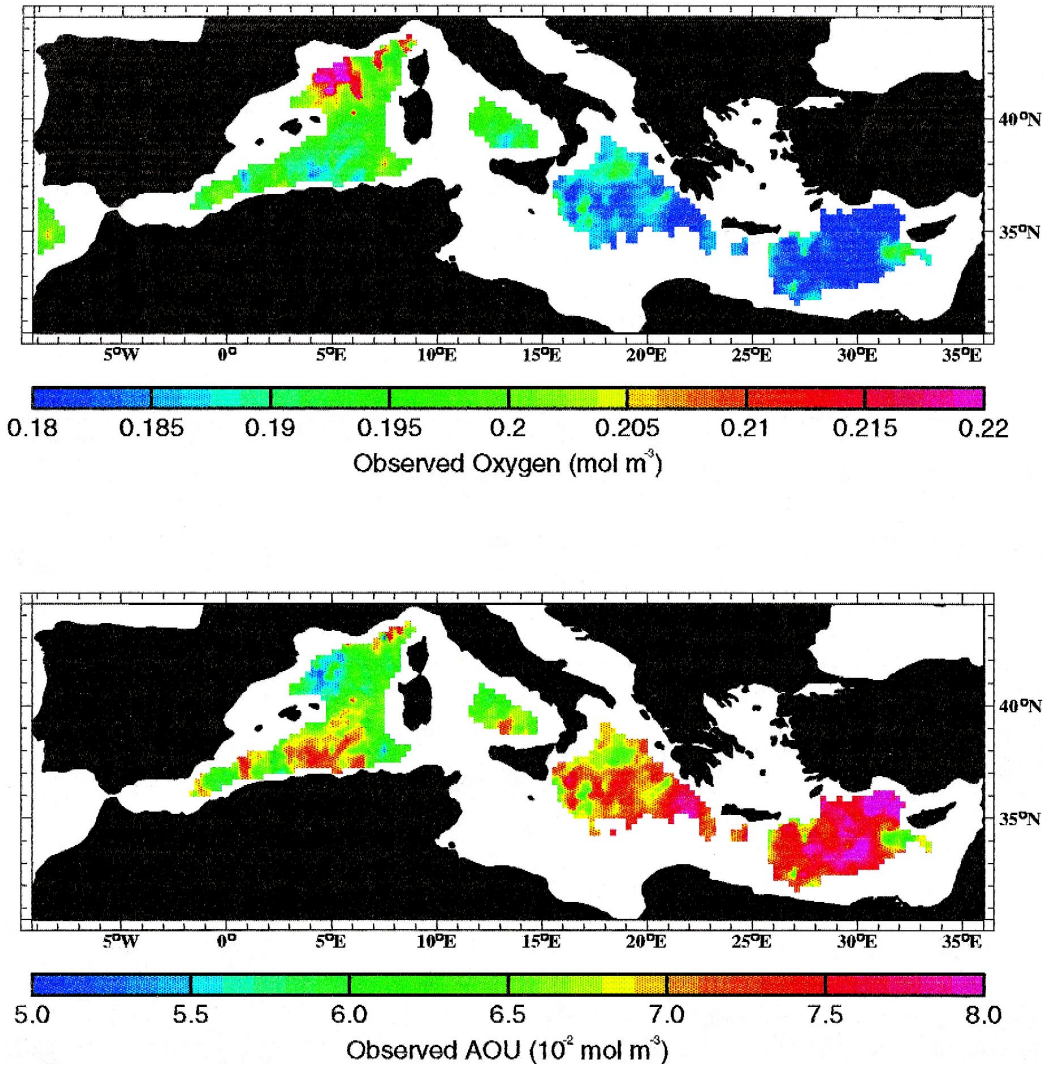

Fig. 1. Annual average observed oxygen and apparent oxygen utilisation (both mol O_2 m^{-3}) on the 1500 m isobath, as derived from MED2 historical database of Brasseur et al. (1996).

the clear signature of deep convection in the Gulf of Lions with concentrations greater than 21 mol O_2 m^{-3}. At this depth in the eastern basin, concentrations are significantly lower, typically less than 19 mol O_2 m^{-3}, with the lowest concentrations appearing off the coast of Turkey in the Levantine basin. For the AOU values the gradient is reversed with the higher values to the south and east, although a broadly similar pattern can be seen.

Fig. 2 shows vertical sections of both the oxygen concentration and the AOU on a transection which passes through both the western and eastern basins. From those regions where data are available (shaded regions represent missing data) it is possible to assess the vertical trends in the two basins. The western basin exhibits a number of pronounced features: deep convection in the Gulf of Lions is clear as a vertically uniform region of high oxygen concentration (greater than 21 mol O_2 m^{-3}) extending to the bottom. Also visible is a clear mid-depth minimum in the oxygen concentration at around 500 m, which appears as a maximum in the AOU picture. No such

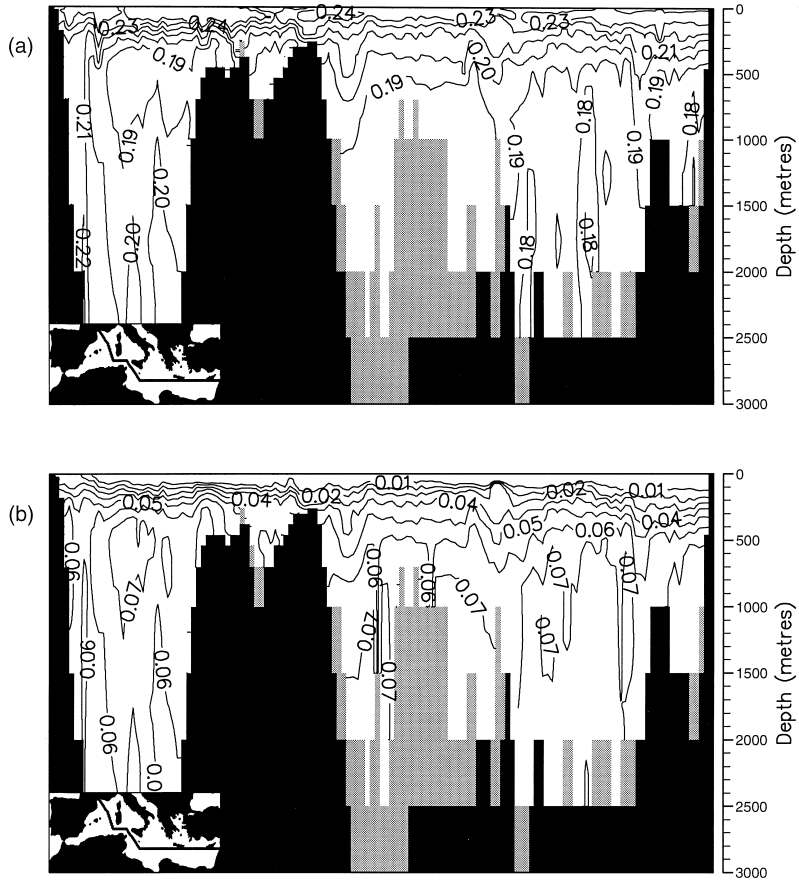

Fig. 2. Annual average observed (a) oxygen and (b) apparent oxygen utilisation (both mol O_2 m^{-3}). The contour interval is 0.01 mol O_2 m^{-3} in both cases. The path of the section is shown in the inset, and passes from the Gulf of Lions in the west to the coast of Turkey in the east. Lightly shaded regions indicate missing data.

mid-depth minimum is present in the eastern part of the section, where the maximum in AOU is generally towards the bottom. Furthermore, in the eastern basin the 0.07 mol O_2 m^{-3} AOU contour is nearest the surface in the Levant, suggesting that the oldest water resides in this part of the basin.

3. Model details

The oxygen and ideal age distributions are modelled using an off-line approach, making use of fields from the GFDL primitive equation model (MOM, see Cox, 1984), to compare with the climatological fields presented in Section 2.

The MOM for the Mediterranean region has been integrated for 100 yr following studies by Pinardi and Navarra (1993), Roussenov et al. (1995) and Wu and Haines (1996). This length of integration is sufficient for the upper and mid-depth circulation to reach equilibrium, but the deep water is ventilated too slowly owing to a number inadequacies in the model circulation, particularly near strong topography (see Haines and Wu, 1998). Instead of renewing bottom waters, ventilation of dense water occurs largely at mid-depth, leading to bottom water which is typically older than water at mid-depth. The model has $0.25° \times 0.25°$ horizontal resolution along with 19 levels in the vertical, the surface layer being 10 m in depth. The Strait of Gibraltar is open allowing an free inflow of Atlantic water and outflow of Mediterranean water. The model is initialised to the Levitus (1982) climatology, and forced by an annual cycle of

monthly mean winds (from National Meteorological Centre data) along with a temperature and salinity relaxation at the surface, a device to maintain realistic temperature/salinity structure within the model. Wu and Haines (1996) employ sufficiently low horizontal viscosity and diffusivity to allow the background flow to become baroclinically unstable, forming eddies on a scale slightly larger than the Rossby radius of deformation (about 15–20 km in the Mediterranean compared with a horizontal resolution of around 20 km). These baroclinic eddies are found to be essential in achieving realistic spreading of water mass properties, particularly for Levantine Intermediate Water, from formation sites.

The off-line tracer integrations employ a single annual cycle of temperature (θ), salinity (S), and mean velocity field ($\boldsymbol{u}$) with a temporal resolution of 5 days. This single annual cycle is formed using output from the final 10 yr of the GCM integration. The oxygen and ideal age models use this annual cycle in conjunction with the appropriate boundary conditions and source/sink terms. The off-line approach provides an effective and efficient way of carrying out a large number of different calculations based on the same model, although at the cost of removing some explicit variability. However, the temporal resolution of 5 days is short enough on the scale of a typical eddy lifetime (perhaps weeks) that a reasonable representation of the eddies is retained. Clearly, to retain variability at all frequencies, one must return to use of the full GCM (albeit with consequent computational penalty).

The equation for the time evolution of a passive tracer in the off-line model is:

$$C_t = -\nabla.(\boldsymbol{u}C) + \kappa_h \nabla_h^2 C + (\kappa_v C_z)_z \qquad (1)$$

where u is the three-dimensional velocity field, while subscripts t and z represent derivatives with respect to time and the vertical co-ordinate respectively. See Williams et al. (1995) for further details of the off-line model. The horizontal diffusivity, κ_h, is chosen to be 50 $m^2\ s^{-1}$, which is close to that implied by the biharmonic diffusion term in the prognostic model, and can compensate for the loss of explicitly variability in some regions. In other regions, the effect of the time-varying flow leads to an up-gradient transfer of tracer and requires an advective parametrisation of the sub-scale such as the scheme of Gent and McWilliams (1990); see, for example in the Mediterranean, Stratford and Williams (1997). The vertical diffusivity, κ_v, is exactly that used in the prognostic model, being 3×10^{-5} $m^2\ s^{-1}$ at the surface, smoothly decreasing towards the bottom.

3.1. Oxygen model

The oxygen concentration is calculated using the off-line tracer model described by Eq. (1), together with additional sources and sinks (as depicted in Fig. 3). The full equation for the time evolution of the oxygen concentration is then:

$$[O_2]_t = -\nabla.(\boldsymbol{u}[O_2]) + \kappa_h \nabla_h^2 [O_2] + (\kappa_v [O_2]_z)_z - (\overline{w'[O_2]'})_z + F_z \qquad (2)$$

Here, $[O_2]_t$ is the time rate of change of the dissolved concentration of oxygen, $\overline{w'[O_2]'}$ is a vertical

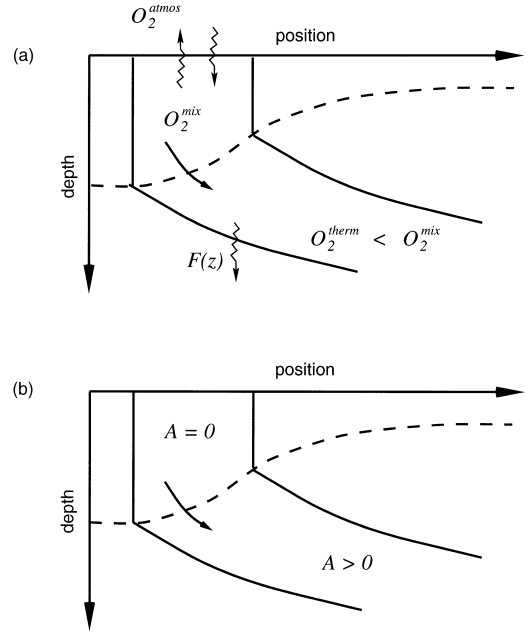

Fig. 3. Schematic diagrams showing the nature of (a) oxygen and (b) the ideal age tracer. Oxygen is exchanged with the atmosphere at the surface, and is transferred through the mixed layer into the interior where the concentration is reduced by consumption, represented by $F(z)$. In comparison, the age tracer is set to zero in the mixed layer (dashed lines) at all times; once subducted, fluid parcels move along isopycnals (solid lines) in the interior where the age increases (linearly in the limit of no mixing).

turbulent flux of oxygen within the mixed layer, and F_z is a term representing the net consumption of oxygen.

The air–sea transfer of oxygen is parametrised according to the mismatch between the surface oxygen concentration $[O_2]_{z=0}$ and the saturated oxygen concentration $[O_2]^{sat}$:

$$\overline{w'[O_2]'}\big|_{z=0} = k_w\left([O_2]^{sat} - [O_2]\right) \quad (3)$$

The saturated oxygen content $[O_2]^{sat}$, a function of

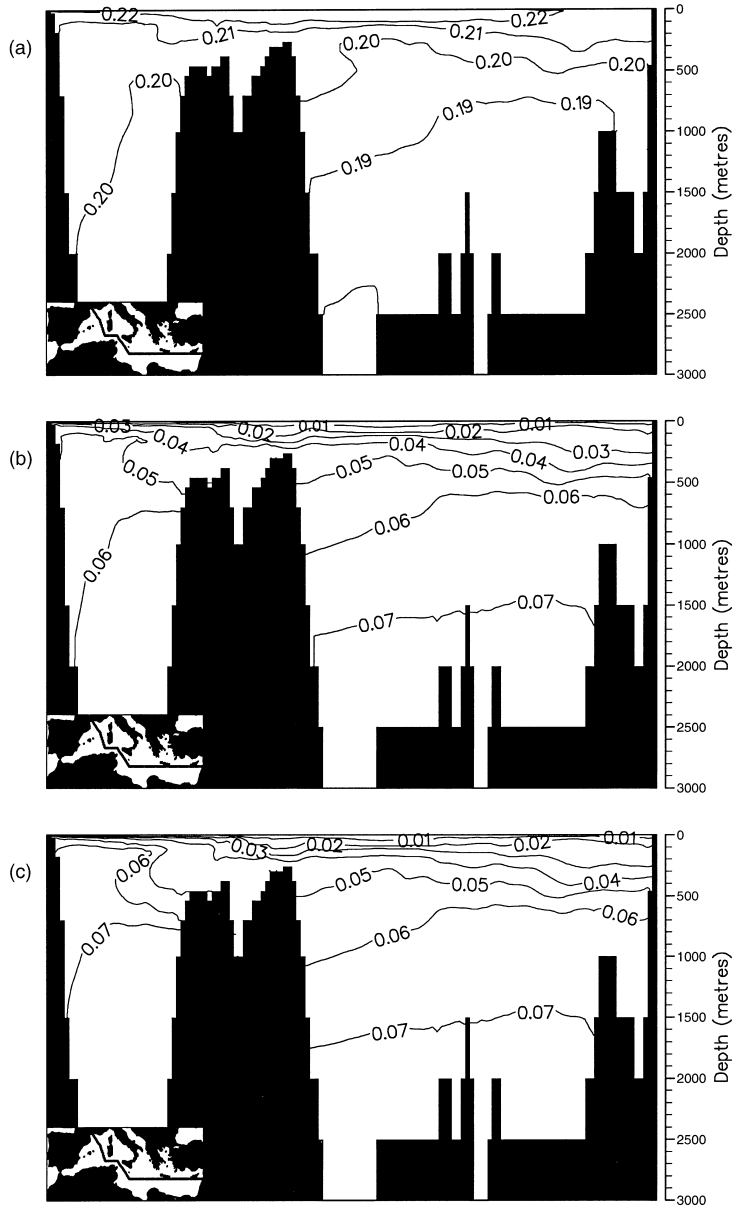

Fig. 4. Model predictions of (a) oxygen concentration (mol O_2 m^{-3}) and (b) apparent oxygen utilisation (mol O_2 m^{-1}) for the case of 12 and 24 g C m^{-2} yr^{-1} new production in the eastern and western basins respectively. In (c), the apparent oxygen utilisation is shown for the increased consumption rate relating to the case of 36 g C m^{-2} yr^{-1} new production in the western basin. The contour interval is 0.01 mol O_2 m^{-3} in all cases.

both temperature and salinity, is calculated from the empirical formula of Weiss (1970) and varies on the 5-day annual cycle following θ and S. A piston velocity, k_w, measuring the equilibration time between air and water, is computed from the empirical relation of Liss and Merlivat (1986) using the monthly NMC wind data (adjusted from 1000 mb to 10 m after Thompson et al., 1983) used to drive the GCM. The magnitude of the piston velocity is typically of order 10^{-5} m s^{-1}, corresponding to an equilibration time of around 30 days for a mixed layer depth of 30 m.

Turbulence within the mixed layer is assumed to homogenise the oxygen concentration vertically, the depth of the mixed layer being identified by an increase in the density of 0.05 kg m^{-3} over the surface value. During periods of mixed-layer deepening, oxygen-poor water is introduced from below,

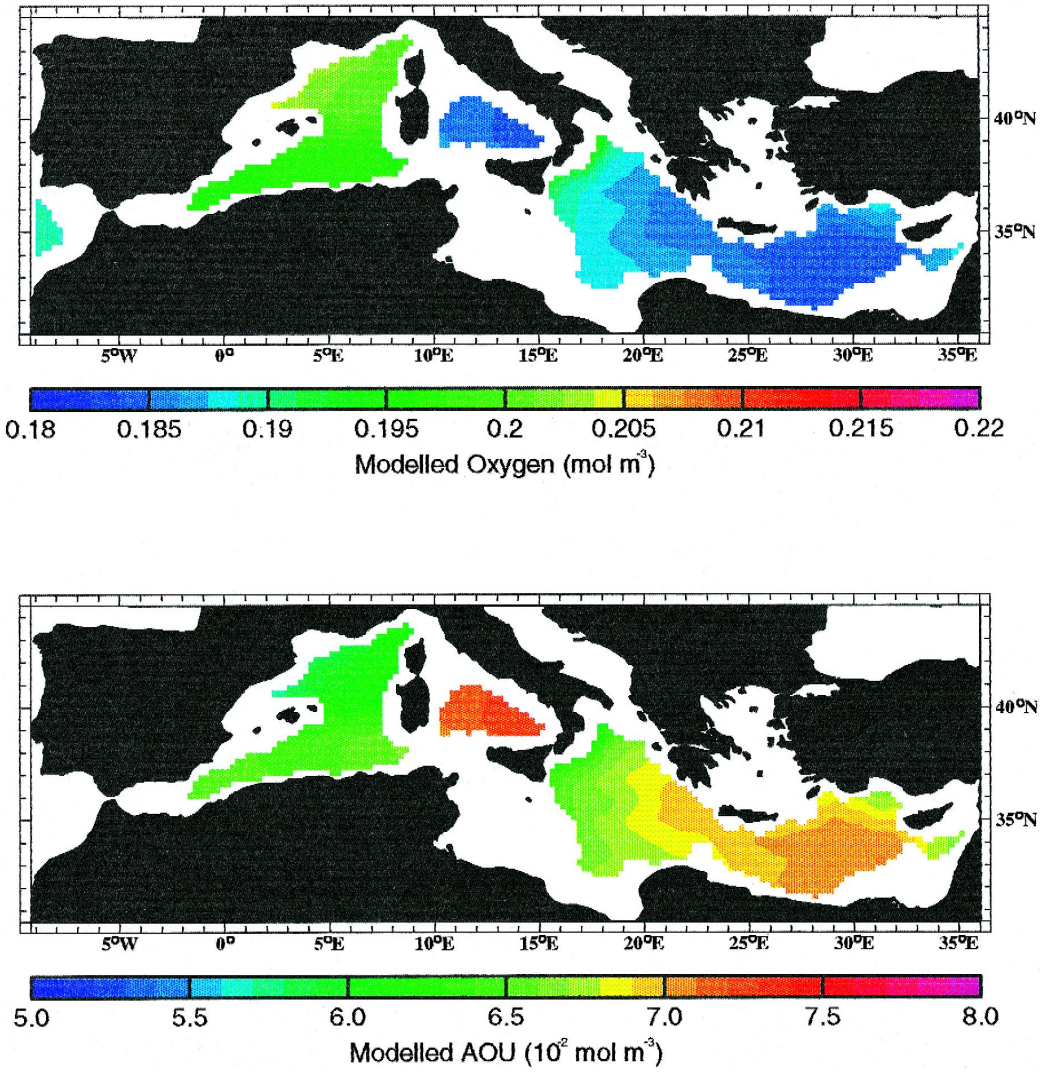

Fig. 5. Model predictions of oxygen concentration and apparent oxygen utilisation (both mol O_2 m^{-3}) on the 1500 m isobath with 12 and 24 g C m^{-2} yr^{-1} new production in the eastern and western basins, respectively.

with an entrainment flux at the base of the mixed layer given by

$$\overline{w'[O_2]}\big|_{z=-h} = H([O_2]_{th} - [O_2]_{z=0})h_t. \quad (4)$$

Here, $[O_2]_{th}$ represents the oxygen concentration of the entrained water from the thermocline, and the Heaviside function, H, is defined to be unity when there is mixed layer deepening with $h_t > 0$, and zero otherwise.

The interior sink of oxygen is represented by the term F_z in Eq. (2), the form of which is based on the empirical parametrisation of Martin et al. (1987) following measurements of particulate nutrient fluxes as a function of depth in the VERTEX experiment in the North Pacific. The divergence of these fluxes is associated with a consumption of oxygen when there is particulate remineralisation, and can be converted to an implied oxygen consumption by multiplication by the appropriate Redfield ratio. In this way the consumption of oxygen can be described by:

$$F_z = F_0(z/z_0)^{\gamma-1} \quad (5)$$

where z_0 is some reference level (100 m) while F_0 and γ are empirically determined parameters. In the VERTEX region, the overall oxygen consumption can be represented to a good approximation by taking $F_0 = 4.7 \times 10^{-10}$ mol O_2 m^{-3} s^{-1} and $\gamma = -0.87$. The new production in the VERTEX area was estimated to be 12 g C m^{-2} yr^{-1}.

We choose to employ the parametrisation Eq. (5) based on the VERTEX region, but adjust the value of the prefactor F_0 according to the local value of the new production. The exact functional form of the parametrisation could be different in the Mediterranean, where the water column is significantly warmer than the Pacific and higher microbial activity might be expected to lead to a more rapid decrease in the consumption rate with depth. For example, Suess (1980) describes a model based on data from different areas of the world ocean in which the oxygen consumption decreases as z^{-2} (compared with $z^{-1.87}$ here). However, the uncertainty in the exact functional form is probably small compared with that in the new production, which determines the value of F_0.

In the eastern Mediterranean, an oligotrophic region like the VERTEX area, new production is estimated to be 12 g C m^{-2} yr^{-1} (Bethoux, 1989), so we adopt the above values of F_0 and γ here. This gives rise to an oxygen utilisation rate of around 0.015 mol O_2 m^{-3} yr^{-1} at 100 m, which is similar to that estimated by Jenkins (1987) for the beta triangle site in the North Atlantic. Estimates of the new production in the western Mediterranean are more wide-ranging: Bethoux (1989) gives 12–36 g C m^{-2} yr^{-1}. In an attempt to address this uncertainty, we have undertaken two off-line oxygen integrations corresponding to new production of 24 and 36 g C m^{-2} yr^{-1}, where the values of F_0 are scaled by a factor of 2 and 3 respectively, while γ is unchanged. The comparison of these two integrations allows the sensitivity of oxygen model to the consumption rate to be assessed.

3.2. Ideal age

The ideal age for a given fluid parcel is defined here as the elapsed time since that fluid was sub-

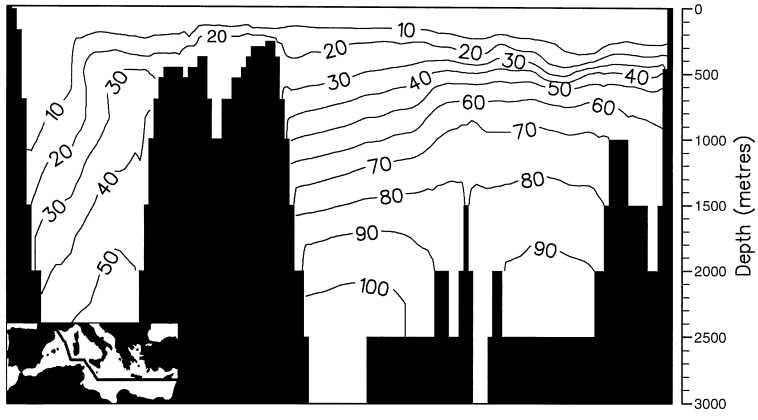

Fig. 6. A transection of modelled age (years). The contour interval is 10 yr.

ducted into the thermocline from the base of the mixed layer (see, for example, Thiele and Sarmiento, 1990). The age, $A(\boldsymbol{x}; t)$, is set to be zero in the mixed layer at all times:

$$A(\boldsymbol{x};t) = 0 \quad (6)$$

while in the interior, the time evolution of A follows Eq. (1) with the appropriate source term included

$$A_t = -\nabla.(\boldsymbol{u}A) + \kappa_h \nabla_h^2 C_z + (\kappa_v C)_z + 1 \quad (7)$$

In an ideal case where there is no mixing in the interior, a fluid parcel leaving the mixed layer will age linearly with time (Fig. 3b).

4. Model results

The initial conditions for the off-line tracer model are a homogeneous constant value, zero in the case of age and 0.1 mol O_2 m^{-3} for oxygen. Integrations of 200 yr have been performed for both the ideal age and oxygen, sufficient for a statistically steady state to be approached. In all cases the result presented will be an annual average from the final year of integration.

4.1. Oxygen distribution

The oxygen results are presented in terms of both absolute oxygen concentration and AOU, where the saturation values of oxygen have been computed from the average model (θ, S) properties.

The modelled oxygen concentration is shown in Fig. 4a for the case in which the new production is 24 g C m^{-2} yr^{-1} in the western basin and 12 g C m^{-2} yr^{-1} in the eastern basin. The modelled oxygen shows higher values in the western basin compared to those in the east, although the contrast of up to 0.015 mol O_2 m^{-3} is typically only half that revealed in the climatology. In the western basin the deep water oxygen concentration is around 0.20 mol O_2 m^{-3} with corresponding AOU (Fig. 4b) values of around 0.06 mol O_2 m^{-3}. However, there is little or no evidence of a mid-depth oxygen minimum as observed in the data. In the eastern basin, the deep water oxygen values are generally 0.18–0.19 mol O_2 m^{-3} with a minimum in the deepest part of the Ionian. There is no oxygen minimum at mid-depth in the eastern basin, which is consistent with the data. Also consistent with the data are lower oxygen concentrations towards the surface in the Levant, suggesting older water upwells in this region.

Fig. 4c shows the model prediction of AOU for the case of the higher consumption in the western basin based on new production of 36 g C m^{-2} yr^{-1}. In the western basin the change in consumption has caused a decrease in the oxygen concentration of roughly 0.01 mol O_2 m^{-3}, with a corresponding increase in the AOU. Even with the increased con-

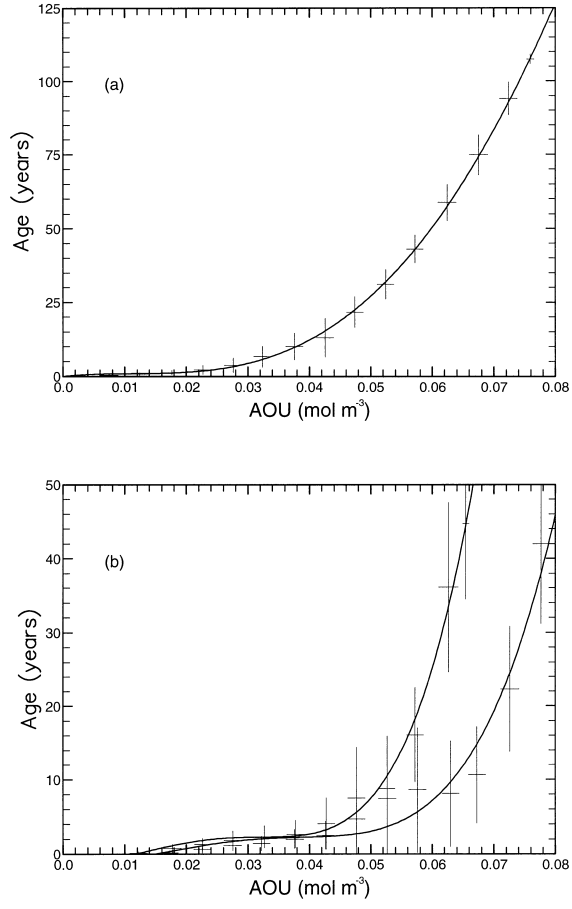

Fig. 7. The AOU relationship for (a) the eastern basin and (b) the western basin, where there are two curves representing the different oxygen utilisation rates relating to 24 and 36 g C m^{-2} yr^{-1} new production; the rightmost is for the case of 36 g C m^{-2} yr^{-1} which gives rise to consistently lower age values for a given AOU. The width of the cross indicates the variance about the mean in each AOU bin.

sumption, the model AOU does not exhibit a mid-depth maximum as is observed (Fig. 2b).

Fig. 5 shows the modelled fields of oxygen concentration and AOU on the 1500 m isobath for the lower consumption rate in the west. Both fields are qualitatively similar to the equivalent climatological fields (Fig. 1), although the model has failed to capture the extremes of high oxygen associated with deep convection in the Gulf of Lions, and the lowest values observed in the Levant. The correlation coefficient between observed AOU and modelled AOU for the whole Mediterranean is 0.87, while that between observed and modelled oxygen is 0.75.

4.2. Modelled age

A transection of age values from the off-line tracer model is shown in Fig. 6, from which it can be seen that in general, water becomes older as depth increases. In the western portion of the section, which passes through the Gulf of Lions, there is some evidence of deep convection with younger water penetrating to mid-depth. However, the modelled deep convection in this region is not reaching the bottom which suggests that the highest ages seen in the western basin ($\sim$ 50 yr) are overestimates.

In the eastern part of the section, which passes to the south of both Crete and Cyprus, considerably older water is observed. At mid-depth, the highest ages ($\sim$ 70 yr) are seen towards the east of the basin, while in the deepest region of the model the situation is reversed with the highest ages ($\sim$ 100 yr) seen in the Ionian, and slightly lower ages in the Levantine. Again, ventilation of bottom water is too weak so that bottom water ages should be younger than those at mid-depth as reflected in higher CFC concentrations in bottom waters observed in the Ionian by Roether and Schlitzer (1991).

4.3. The AOU–age relationship

The model results presented above suggest that increasing AOU is associated with older water. In order to quantify this relationship the results for AOU and age from each position in the model have been binned according to the AOU value. The means of the values for each AOU bin (width 5×10^{-3} mol O_2 m^{-3}) are computed, along with the standard deviations to measure the variance. These values are indicated by the error bars in Fig. 7, which are 2 standard deviations in extent.

For the eastern basin (Fig. 7a) there is a clear monotonic increase in the age with increasing AOU. A simple polynomial fit has been drawn through the points. For a given AOU value, the variance in the model age is typically 10–15 yr. In the western basin (Fig. 7b) results are plotted for both the higher and lower consumption cases. The higher consumption rate (based on 36 g C m^{-2} yr^{-1} new production) gives lower ages for a given AOU. However, in both cases the variance in the age values associated with a given AOU is large: 15–20 yr in the higher AOU

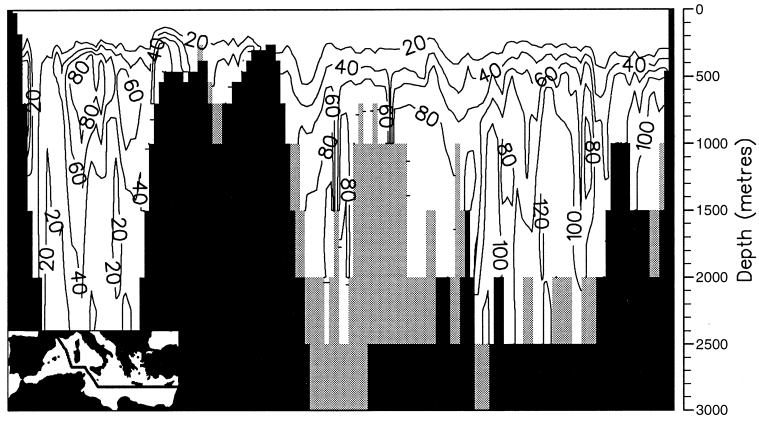

Fig. 8. A transection of age computed using the observed AOU field and the modelled AOU–age relationship. The contour interval is 20 yr. Lightly shaded regions again indicate missing data.

range. The difference between the two consumption cases is even larger for AOU values beyond 0.06 mol O_2 m^{-3}.

Using the AOU–age relationships for the east and the west (with the lower consumption rate), an age value can be recovered from the climatological AOU values. The resulting transection is shown in Fig. 8, suggesting that the age of the deep water is around 20–40 yr and 80–120 yr in the western and eastern basins respectively. However, values for the age at mid-depth in the western basin where the observed AOU exceeds 0.06 mol O_2 m^{-3} are clearly unreliable, reflecting the large difference seen between the curves in Fig. 7b.

5. Discussion and Conclusion

Climatological oxygen distributions reveal greater oxygen concentration at depth in the western Mediterranean, when compared with the eastern Mediterranean. This oxygen distribution reflects the enhanced ventilation of the western basin, since the higher new production in the western Mediterranean tends to reduce the oxygen concentration at depth. In this way, the oxygen distribution is providing a qualitative measure of the age of fluid, defined as elapsed time since fluid is at the surface. However, obtaining a more quantitative measure of the age is difficult, as the circulation pathways and mixing rates are not well known.

In this study, we attempt to deduce the age distribution from the climatological oxygen distribution by using a functional relationship between apparent oxygen utilisation (AOU) and age derived from off-line tracer integrations in the Mediterranean. The ideal age integration shows ages reaching up to 100 yr in the eastern basin and up to 50 yr in the western basin, although deep convection should be more active in the model. The oxygen model includes air–sea transfer of oxygen, entrainment, advection and an interior loss through consumption (that is enhanced in the western basin owing to the higher new production there). The model produces an oxygen distribution that captures the gross features of the climatology, apart from the oxygen minimum at mid-depths in the western basin, which is caused by deep convection being underestimated. The correlation between the observed and modelled AOU is 0.87, while between observed and modelled oxygen it is 0.75. The functional relationship between AOU and age obtained from the model shows the expected increase in AOU with age, but the exact form of the relationship differs in each basin. The different choices in oxygen utilisation rate in the western basin modify the AOU–age relationship and lead to an offset of at least 20 yr for higher values of AOU.

Using the separate functional relationships for the western and eastern basins leads to predictions for the climatological age reaching 80–120 and 20–40 yr at the bottom of the eastern and western Mediterranean respectively. There are a number of significant sources of error to be considered in this approach. First, the variance in the AOU–age relationship as measured by the error bars in Fig. 7 suggests an error of around 10–15 yr in the eastern basin and 15–20 yr in the western basin. Second, the choice of oxygen utilisation rate, which is here related to the new production, alters the model relationship as seen in Fig. 7b. The new production in the western basin is estimated by Bethoux (1989) to be 12–36 g C m^{-2} yr^{-1}, while in the eastern basin to be 12 g C m^{-2} yr^{-1} with an uncertainty of perhaps ± 6 g C m^{-2} yr^{-1}. Therefore, the error in the recovered age in the western basin will be perhaps 40 yr, whereas in the eastern basin it will be smaller, around 20 yr. However, an age estimate for the bottom water of 20–40 yr in the west turns out to be quite reasonable, although a reliable estimate is made difficult by the problems with deep convection.

In comparison, Ovchinnikov et al. (1985) estimate an overturning timescale for the eastern basin of 70 yr, and for the western basin of 40 yr. Roether and Schlitzer (1991) use tritium/helium and CFC observations to deduce a renewal timescale of 120–130 yr for the deep waters in the eastern basin. Our recovered ages are broadly consistent with these independent estimates. It should be noted that the present work takes no account of changes in the deep circulation recently observed by Roether et al. (1995), which suggest Aegean deep water formation gives rise to a more rapid renewal timescale of perhaps 30–40 yr. New GCM integrations would be required to try to address such variability.

The accuracy of biogeochemical tracer modelling is clearly limited by a number of factors. The impor-

tance of a credible physical simulation is highlighted by the problems with deep convection in the present model, which has a large effect on the oxygen concentrations and ages of the deep water. Experimental measurements of new production are also uncertain, although an oxygen model could be used to try to discriminate between different estimates. The combined oxygen–age approach was adopted to try to overcome the deficiencies exhibited by the individual tracer models, and shows a degree of success in estimating the overturning timescale. Finally, we note that this approach could be adopted in other regions of the world ocean provided dynamical and tracer models can be adapted successfully to local conditions. This approach could be useful in parts of the world ocean to which anthropogenic tracers have not penetrated.

Acknowledgements

The authors would like to thank Keith Haines and Peili Wu for providing their version of the Mediterranean model code (MOM). We are also grateful to two anonymous reviewers for helpful comments. This work was funded by the European Community MAST programme under grants MAS2-CT-0055 (MERMAIDS) and MAS3-CT95-0043 (CLIVAMP).

References

Bethoux, J.P., 1989. Oxygen consumption, new production, vertical advection and environment evolution in the Mediterranean sea. Deep-Sea Res. 36, 769.

Brasseur, P., Beckers, J.M., Brankart, J.M., Schoenauen, R., 1996. Seasonal temperature and salinity fields in the Mediterranean Sea: climatological analyses of an historical data set. Deep-Sea Res. 43, 159.

Cox, M.D., 1984. A primitive equation, three-dimensional model of the ocean. GFDL ocean group technical report no. 1, 1984. Geophysical Fluid Dynamics Laboratory, Princeton University, USA.

Gent, P.R., McWilliams, J.C., 1990. Isopycnal mixing in ocean circulation models. J. Phys. Oceanogr. 20, 150–155.

Haines, K., Wu, P., 1998. GCM studies of intermediate and deep waters in the Mediterranean. J. Mar. Syst. 18, 197–214.

Jenkins, W.J., 1987. ^{3}H and ^{3}He in the beta triangle: observations of gyre ventilation and oxygen utilization rates. J. Phys. Oceanogr. 17, 763–783.

Levitus, S., 1982. Climatological atlas of the world ocean. NOAA Prof. Pap. 13. U.S. Govt. Print. Off., Washington, DC, 173 pp.

Liss, P.S., Merlivat, L., 1986. Air–sea gas exchange rates: introduction and synthesis. In: Baut-Ménard, P. (Ed.), The Role of Air–Sea Exchange in Geochemical Cycling, Reidel, 1986, pp. 113–127.

Martin, J.H., Knauer, G.A., Karl, D.M., Broenkow, W.W., 1987. VERTEX: carbon cycling in the northeast Pacific. Deep-Sea Res. 34, 267–285.

Ovchinnikov, I.M., Zats, V.I., Krivosheya, V.G., Udodov, A.I., 1985. Formation of deep eastern Mediterranean waters in the Adriatic Sea. Oceanology 25, 704–707.

Pinardi, N., Navarra, A., 1993. Baroclinic wind adjustment processes in the Mediterranean Sea. Deep-Sea Res. II 40, 1299–1326.

Roether, W.R., Schlitzer, R., 1991. Eastern Mediterranean deep water renewal on the basis of chlorofluoromethane and tritium data. Dyn. Atmos. Oceans 15, 333–354.

Roether, W.R., Manca, B., Klein, B., Bregant, D., Georgopoulos, D., 1995. Eastern Mediterranean deep waters found in an entirely new state. Science 271, 333–335.

Roussenov, V., Stanev, E., Artale, V., Pinardi, N., 1995. A seasonal model of the Mediterranean Sea general circulation. J. Geophys. Res. 100, 13515–13538.

Stratford, K., Williams, R.G., 1997. A tracer study of the formation, dispersal, and renewal of Levantine Intermediate Water. J. Geophys. Res. 102, 12539–12549.

Suess, E., 1980. Particulate organic carbon flux in oceans—surface productivity and oxygen utilisation. Nature 288, 260–263.

Thiele, G., Sarmiento, J.L., 1990. Tracer dating and ocean ventilation. J. Geophys. Res. 95, 9377–9391.

Thompson, K.R., Marsden, J.L., Wright, D.G., 1983. Estimation of low-frequency wind stress fluctuations over the open ocean. J. Phys. Oceanogr. 13, 1003–1011.

Weiss, R.F., 1970. The solubility of nitrogen, oxygen and argon in water and seawater. Deep-Sea Res. 17, 721–735.

Williams, R.G., Spall, M.A., Marshall, J.C., 1995. Does Stommel's mixed-layer 'Demon' work?. J. Phys. Oceanogr. 25, 3089–3102.

Wu, P., Haines, K., 1996. A modelling study of deep water formation in the Mediterranean. J. Geophys. Res. 101, 6591–6607.

Wüst, G., 1935. Schichtung und Zirkulation des Atlantischen Ozeans. Die Stratosphäre. In: Wissenschaftliche Ergebnisse der Deutschen Atlantischen Expedition auf dem Forschungs— und Vermessungsscschiff 'Meteor' 1925–1927, 6: 1st Part, 2, 180 pp.